The Astrophysical Journal, 807:163 (8pp), 2015 July 10 doi:10.1088/0004-637X/807/2/163

GRB 080503 LATE AFTERGLOW RE-BRIGHTENING: SIGNATURE OF A MAGNETAR-POWERED MERGER-NOVA

He Gao[1,2,3,4], Xuan Ding[1], Xue-Feng Wu[1,5], Zi-Gao Dai[6,7], and Bing Zhang[8]
[1] Purple Mountain Observatory, Chinese Academy of Sciences, Nanjing 210008, China; hug18@psu.edu, xfwu@pmo.ac.cn
[2] Department of Astronomy and Astrophysics, Pennsylvania State University, 525 Davey Laboratory, University Park, PA 16802, USA
[3] Department of Physics, Pennsylvania State University, 525 Davey Laboratory, University Park, PA 16802, USA
[4] Center for Particle and Gravitational Astrophysics, Institute for Gravitation and the Cosmos, Pennsylvania State University, 525 Davey Laboratory, University Park, PA 16802, USA
[5] Joint Center for Nuclear Particle Physics and Cosmology, Purple Mountain Observatory-Nanjing University, Nanjing 210008, China
[6] School of Astronomy and Space Science, Nanjing University, Nanjing 2100093, China; dzg@nju.edu.cn
[7] Key Laboratory of Modern Astronomy and Astrophysics (Nanjing University), Ministry of Education, China
[8] Department of Physics and Astronomy, University of Nevada Las Vegas, NV 89154, USA; zhang@physics.unlv.edu
Received 2015 January 21; accepted 2015 May 24; published 2015 July 9

ABSTRACT

GRB 080503 is a short gamma-ray burst (GRB) detected by *Swift* and has been classified as a GRB originating from a compact star merger. The soft extended emission and the simultaneous late re-brightening in both the X-ray and optical afterglow light curves raise interesting questions regarding its physical origin. We show that the broadband data of GRB 080503 can be well explained within the framework of the double neutron star merger model, provided that the merger remnant is a rapidly rotating massive neutron star with an extremely high magnetic field (i.e., a millisecond magnetar). We show that the late optical re-brightening is consistent with the emission from a magnetar-powered "merger-nova." This adds one more case to the growing sample of merger-novae associated with short GRBs. The soft extended emission and the late X-ray excess emission are well connected through a magnetar dipole spin-down luminosity evolution function, suggesting that direct magnetic dissipation is the mechanism to produce these X-rays. The X-ray emission initially leaks from a hole in the merger ejecta pierced by the short GRB jet. The hole subsequently closes after the magnetar spins down and the magnetic pressure drops below ram pressure. The X-ray photons are then trapped behind the merger-nova ejecta until the ejecta becomes optically thin at a later time. This explains the essentially simultaneous re-brightening in both the optical and X-ray light curves. Within this model, future gravitational-wave sources could be associated with a bright X-ray counterpart along with the merger-nova, even if the short GRB jet beams away from Earth.

Key words: gamma-ray burst: general – radiation mechanisms: non-thermal – stars: neutron

1. INTRODUCTION

The frequency range of the next generation gravitational-wave (GW) detectors, such as Advanced LIGO (Abbott et al. 2009), Advanced VIRGO (Acernese et al. 2008) and KAGRA (Kuroda 2010) interferometers, is designed to uncover the final inspiral and merger of compact object binaries (NS–NS, NS–BH, and BH–BH systems). Due to the faint nature of GW signals, an associated electromagnetic (EM) emission signal coinciding with a GW signal in both trigger time and direction could play a crucial role in confirming the astrophysical origin of the GW signals and studying the astrophysical origin of the GW sources (e.g., host galaxy, distance, etc.).

Short-duration γ-ray bursts (SGRBs) have long been proposed to originate from mergers of compact object binaries (Paczýnski 1986, 1991; Eichler et al. 1989; Narayan et al. 1992). If so, SGRBs may provide the brightest EM counterpart associated with events detected by those upcoming interferometers. However, observations of SGRBs suggest that at least some of them are collimated into a small opening angle (Burrows et al. 2006; de Pasquale et al. 2010), so most GW signals would not be detected together with SGRBs (e.g., Metzger & Berger 2012). Lately, additional EM signatures of compact binary mergers (especially for NS–NS systems) have become a topic of growing interest (see Berger 2014 for a review).

Numerical simulations show that a mildly isotropic, sub-relativistic outflow could be ejected during the merger of binary neutron stars, including the tidal tail matter during the merger and the matter from the accretion disk (e.g., Rezzolla et al. 2011; Bauswein et al. 2013; Hotokezaka et al. 2013; Rosswog et al. 2013). The typical mass and speed of the ejecta are in the range of $10^{-4}-10^{-2}\,M_{\odot}$ and $0.1-0.3c$, respectively (Hotokezaka et al. 2013). Recently, several interesting EM signatures from the ejecta whose brightness are essentially determined by the properties of the leftover remnant from the merger.

Usually, the merger product is assumed to be either a black hole or a temporal hyper-massive neutron star that survives 10–100 ms before collapsing into the black hole (e.g., Rosswog et al. 2003, 2013; Aloy et al. 2005; Shibata et al. 2005; Rezzolla et al. 2011). In this case, an optical/infrared transient is expected to be powered by radioactive decay from r-process radioactive material (Li & Paczyński 1998; Kulkarni 2005; Metzger et al. 2010; Barnes & Kasen 2013); henceforth, we call it an r-process-powered merger-nova.[9] Besides this thermal emission, long-lasting radio emission is also expected from the interaction between the ejecta and the ambient medium, although it is normally too weak to be detected (Nakar & Piran 2011; Metzger & Berger 2012; Piran et al. 2013). Such transients are more isotropic than SGRBs. Depending on the direction of our line of sight, these transients could be detected alone or to be accompanied by SGRBs, provided that their

[9] It is named a "macro-nova" by Kulkarni (2005) due to its sub-supernova luminosity, or "kilo-nova" by Metzger et al. (2010) due to its luminosity being roughly $\sim 10^3$ times the nova luminosity.

luminosities are large enough (Metzger & Berger 2012). After several years of searching (Bloom et al. 2006; Perley et al. 2009; Kocevski et al. 2010), an r-process-powered merger-nova was finally claimed to be detected in the infrared band with the *Hubble Space Telescope* (*HST*) for GRB 130603B (Tanvir et al. 2013; Berger et al. 2013). More recently, Yang et al. (2015) re-examined the late afterglow data of GRB 060614 observed with *HST*, and found a significant F814W-band excess at $t \sim 13.6$ days after the burst. They claimed that it is very likely another candidate r-process-powered merger-nova. For both cases, the merger-nova interpretation was based on one single data point.

Alternatively, it has long been proposed that the post-merger product could be a stable or super-massive millisecond magneter if the equation of state of nuclear matter is stiff enough and the total mass of the two neutron stars is small enough (Dai et al. 2006; Fan & Xu 2006; Gao & Fan 2006; Giacomazzo & Perna 2013; Zhang 2013). Evidence of a magnetar following some SGRBs has been collected in the *Swift* data, including the extended emission (Norris & Bonnell 2006; Metzger et al. 2008), X-ray flares (Barthelmy et al. 2005; Campana et al. 2006), and more importantly, "internal plateaus" with rapid decay at the end of the plateaus (Rowlinson et al. 2010, 2013; Lü et al. 2015). Nonetheless, available observations (e.g., the lower limit of the maximum mass of Galactic NSs and the total mass distribution of Galactic NS–NS binaries) and numerical simulations allow the existence of the post-merger massive NS remnant (Zhang 2013; Metzger & Piro 2014, and references therein). Compared with the black hole merger remnants, the main consequences of magnetar merger remnants include the following:

1. the spin-down of the NS remnant supplies an additional energy source to the system;
2. the strong neutrino-driven wind from the NS provides additional mass outflow to the system.

In this case, the detectable EM signatures from the system become much richer. Besides the putative short gamma-ray burst (GRB) signature, the following EM signals may be expected. First, the magnetar would eject a near-isotropic Poynting-flux-dominated outflow, the dissipation of which could power a bright early X-ray afterglow (Zhang 2013). Second, the thermal emission from the ejecta could be significantly enhanced due to additional heating from magnetar wind (Yu et al. 2013; Metzger & Piro 2014). This power could exceed the r-process power, so we may call the corresponding transient a "magnetar-powered merger-nova." Finally, the magnetar power would energize and accelerate the ejecta to a mildly or even moderately relativistic speed, and the interaction between the ejecta and the ambient medium could produce a strong external shock that gives rise to bright broadband emission (i.e., the double neutron star (DNS) merger afterglow model, Gao et al. 2013a). Some recently discovered transients could be interpreted within such a scenario, lending support to a post-merger magnetar remnant. For instance, the Palomar Transient Factory (PTF) team recently reported the discovery of a rapidly fading optical transient source, PTF11agg. Lacking a high-energy counterpart, it has been proposed to be a good candidate for the DNS merger afterglow emission (Wu et al. 2014). Some rapidly evolving and luminous transients discovered recently with the Pan-STARRS1 Medium Deep Survey were proposed to be good candidates of magnetar-powered merger-nova (Yu et al. 2015). Moreover, considering its broadband data, GRB 130603B and its claimed "kilo-nova" can be interpreted within the framwork of a magnetar-powered DNS merger remnant given that the magnetar underwent significant energy loss through GW radiation (Fan et al. 2013b; Metzger & Piro 2014).

Similar to GRB 130603B, GRB 080503 is an SGRB with bright extended emission. Based on its negligible spectral lag of prompt emission and extremely faint afterglow, GRB 080503 has been classified as a GRB[10] originating through a compact star merger (Perley et al. 2009). The most peculiar feature in GRB 080503 is that after the prompt emission (beginning with a short spike and followed by extended emission) and the early steep decay afterglow phase, it did not immediately enter into the regular afterglow phase. Being signalless for about one day, it presented a surprising re-brightening in both the optical and X-ray bands. In the optical, it remained bright for nearly five days. The scenario that the post-merger remnant is a black hole has been investigated for GRB 080503. An "r-process-powered merger-nova" model can marginally explain the optical data, but the X-ray data could not be interpreted (Perley et al. 2009; Hascoët et al. 2012). In this work, we make a comprehensive analysis of the multi-band observations of GRB 080503 and suggest that the magnetar merger remnant scenario can interpret the entire data set, making a solid case to connect the late optical excess of GRB 080503 with a magnetar-powered merger-nova. We note that the idea that GRB 080503 is a good candidate for a magnetar-powered transient has been qualitatively proposed by Metzger & Piro (2014).

2. OBERVATIONAL FEATURES OF GRB 080503

GRB 080503 was detected by the Burst Alert Telescope (BAT) on board the *Swift* satellite at 12:26:13 on 2008 May 3 (see observational details in Perley et al. 2009). Its prompt emission (in the 15–150 keV bandpass) contains a short bright initial spike with a duration of 0.32 ± 0.07 s, followed by soft extended emission lasting for 232 s. The peak flux of the initial spike (measured in a 484 ms time window) and the fluence of the extended emission (measured from 5 to 140 s after the BAT trigger) are $(1.2 \pm 0.2) \times 10^{-7}$ erg cm^{-2} s^{-1} and $(1.86 \pm 0.14) \times 10^{-6}$ erg cm^{-2}, respectively. Although the fluence ratio between the extended emission and the spike is as large as 30 in 15−150 keV, Perley et al. (2009) further analyzed its hardness ratio and spectral lag in detail and found that this burst is still more reminiscent of a GRB originating through a compact star merger.

After the extended emission phase, the X-ray light curve decays rapidly ($\alpha = 2$–4, where $F_\nu \propto t^{-\alpha}$) until it is below the XRT detection threshold, and remains undetectable for about 1 day (as shown in Figure 2). Then the X-ray flux re-brightened to the level of 10^{-3} μJy around 10^5 s after the BAT trigger. Twenty days later, the *Chandra X-Ray Observatory* ACIS-S was again employed to conduct imaging on the relevant position, but no source was detected.

In the optical band, many facilities were employed to search for afterglow signals on the first night after the trigger, such as the *Swift* UV–Optical Telescope, Keck-1 telescope, and Gemini-North telescope; only a single Gemini *g*-band detection was obtained at 0.05 days. However, on the second night after

[10] The physical category of a GRB may not always be straightforwardly inferred based on the duration information, and multi-band observational criteria are needed (Zhang et al. 2009).

the trigger, the afterglow surprisingly rose above the detection threshold to the level of 10^{-1} μJy and remained bright for nearly five days. Later on, the localization region was observed with *HST* in two epochs on 2008 May 12 and July 29. Although only upper limits were achieved, the results infer a rapid decay feature for the late optical excess component.

During the observation, many attempts to measure the redshift of GRB 080503 were made, even with *HST*. Unfortunately, only an upper limit, $z < 4$, was achieved.

3. MODEL DESCRIPTION

3.1. General Picture

If the equation of state of nuclear matter is stiff enough, the central product for a binary neutron star merger could be a stable or a supra-massive NS rather than a black hole. This newborn massive NS would be rotating with a rotation period on the order of milliseconds (close to the centrifugal break-up limit), and may also contain a strong magnetic field $B \gtrsim 10^{14}$ G similar to "magnetars" (Zhang 2013; Metzger & Piro 2014, and reference therein). The millisecond magnetar is surround by a sub-relativistic ($v_{\rm ej} \sim 0.1-0.3c$) ejecta with mass $\sim(10^{-4}-10^{-2})M_\odot$ (Hotokezaka et al. 2013). Considering a variety of origins for the ejecta materials, a spherical symmetry could be reasonably assumed for the ejecta (Metzger & Piro 2014).

Shortly after formation, the magnetar would be surrounded by a centrifugally supported accretion disk (Metzger et al. 2008; Dessart et al. 2009; Lee et al. 2009; Fernández & Metzger 2013), launching a short-lived ($\lesssim s$) collimated jet (Zhang & Dai 2008, 2009, 2010). The jet could easily punch through the ejecta shell and then power the prompt short spike emission and the broadband GRB afterglow emission (Metzger et al. 2008). After the whole jet passes through, it is possible that the gap remains open as the Poynting-flux-dominated magnetar wind continuously penetrates through the hole. Due to the dynamical motion of the ejecta, the ejecta materials tend to quench the outflow by closing the gap. During the early spin-down phase when the Poynting-flux luminosity is essentially a constant, the ram pressure of the ejecta may be balanced by the magnetic pressure of the outflow. After the characteristic spin-down timescale $t_{\rm sd}$, the magnetic pressure drops quickly, and the gap is closed on a timescale of $t_{\rm close}$. The total duration when the magnetar wind leaks from the ejecta and creates bright X-ray emission due to internal dissipation (e.g., through an internal-collision-induced magnetic reconnection and turbulence process; Zhang & Yan 2011) is the duration of the extended emission, i.e., $t_{\rm ee} = t_{\rm sd} + t_{\rm close}$. According to a more detailed estimate (see the appendix for details), this duration could be consistent with the observed duration of extended emission given reasonable parameters. After $t_{\rm ee}$, the magnetar wind is stifled behind the ejecta, so soft extended emission stops and the high-latitute emission in X-ray band shows up, which creates a rapidly dropping X-ray tail (Kumar & Panaitescu 2000; Zhang et al. 2007, 2009). This is similar to the situation when the central engine is shut down.

Trapped by the ejecta materials, the magnetar continuously spins down, and when the magnetar wind encounters the ejecta, a significant fraction of the wind energy (parameterized as ξ) could be deposited into the ejecta, either via direct energy injection by a Poynting flux (Bucciantini et al. 2012), or due to heating from the bottom by the photons generated in a dissipating magnetar wind via forced reconnection (if $R < R_{\rm dis}$) or self-dissipation (if $R > R_{\rm dis}$; Zhang 2013). Such a continuous energy injection not only heats the ejecta material to power the merger-nova (Yu et al. 2013; Metzger & Piro 2014), but also accelerates the ejecta to a mildly or moderately relativistic speed, giving rise to strong afterglow emission by driving a strong forward shock into the ambient medium (Gao et al. 2013a). Note that the remaining fraction of the wind energy $(1-\xi)$ would be stored in the trapped dissipation photons and eventually diffuse out with a deducing factor $e^{-\tau}$, where τ is the optical depth of the ejecta.

In summary, there are four emission sites and several emission components involved in this model (as shown in Figure 1): (i) the jet component that powers the short spike in prompt emission and the GRB afterglow emission; (ii) the early magnetar wind component that powers the soft extended emission and the high latitude tail emission; (iii) the magnetar-powered merger-nova emission component and the corresponding DNS merger afterglow emission; and (iv) the late magnetar-wind-powered X-ray component when the ejecta becomes transparent. In the following, we describe the details for calculating these main emission components.

3.2. Magnetar Wind Dissipation

Considering a millisecond magnetar with an initial spin period $P_{\rm i}$ and a dipolar magnetic field strength B, its total rotational energy reads $E_{\rm rot} = (1/2)I\Omega_0^2 \simeq 2\times10^{52} I_{45} P_{\rm i,-3}^{-2}$ erg (with $I_{45}\sim 1.5$ for a massive neutron star). The spin-down luminosity of the magnetar as a function of time could be expressed as

$$L_{\rm sd} = L_{\rm sd,i}\left(1+\frac{t}{t_{\rm sd}}\right)^{-2} \quad (1)$$

where

$$L_{\rm sd,i} = 10^{47}\, R_{\rm s,6}^6 B_{14}^2 P_{\rm i,-3}^{-4}\ {\rm erg\ s^{-1}} \quad (2)$$

is the initial spin-down luminosity and

$$t_{\rm sd} = 2\times10^5\, R_{\rm s,6}^{-6} B_{14}^{-2} P_{\rm i,-3}^2\ {\rm s} \quad (3)$$

is the spin-down timescale. Hereafter, the convention $Q_x = Q/10^x$ is adopted in cgs units.

The spin-down luminosity is essentially carried by a nearly isotropic Poynting-flux-dominated outflow. In the free zone (e.g., in the direction of the cavity drilled by the jet or the intrinsically open regions in the ejecta), the magnetar wind would leak out from the ejecta and undergo strong self-dissipation beyond $R_{\rm dis} > R_{\rm ej}$, giving rise to extended emission (along the jet direction) or a bright X-ray afterglow emission (off-axis direction; Zhang 2013). In the confined wind zone, the magnetar wind is expanding into the ejecta and the magnetic energy may be rapidly discharged via forced reconnection (if $R < R_{\rm dis}$) or self-dissipation (if $R > R_{\rm dis}$). The trapped dissipation photons would eventually show up when the ejecta became optically thin.

As a rough estimation, one can assume an efficiency factor η_ν to convert the spin-down luminosity to the observed luminosity at frequency ν, so that one has

$$F_\nu \sim \frac{\eta_\nu L_{\rm sd}}{4\pi\nu D_L^2}. \quad (4)$$

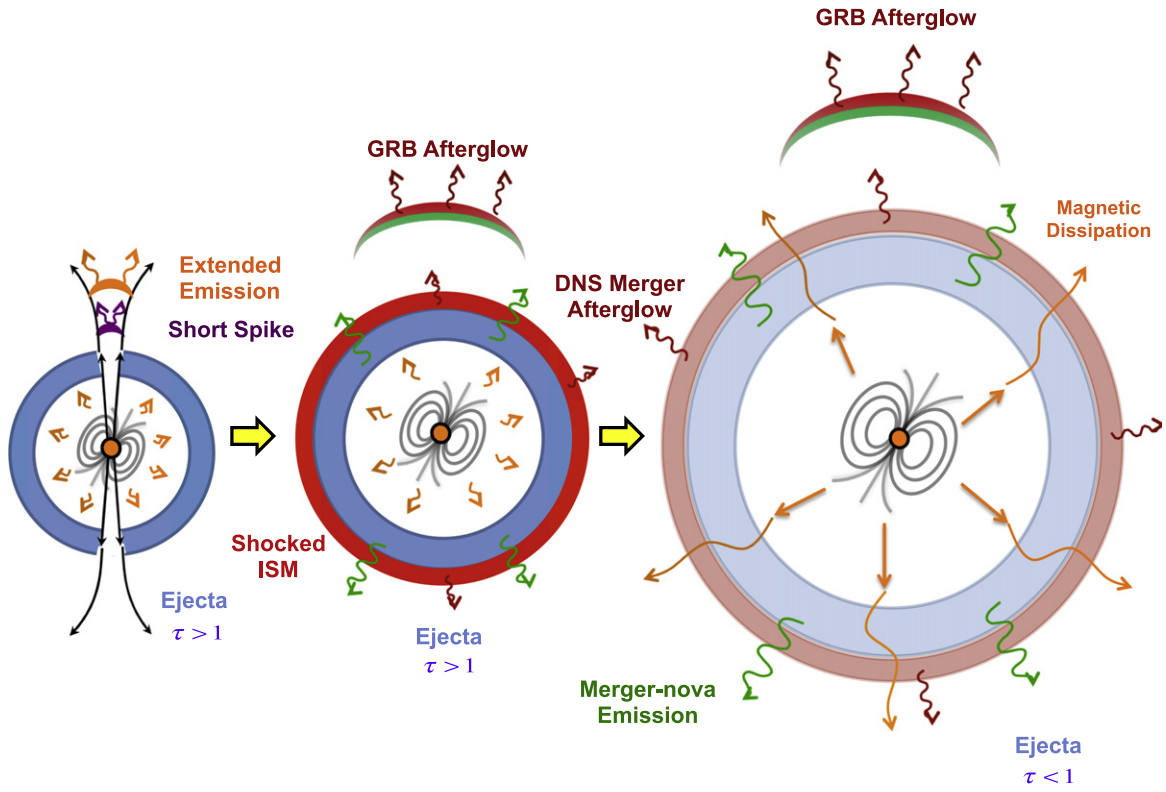

Figure 1. Cartoon picture of the model, illustrating various emission sites and emission components at different stages, from an NS–NS merger event that results in a stable millisecond magnetar remnant. In the early stage, a short-lived jet was launched, punching through the ejecta shell and giving rise to the prompt short spike emission. Following the jet, the magnetar wind leaks out through the opening gap, dissipates at a larger radius, and powers the extended emission. In the intermediate stage, the magnetar spins down and the ram pressure overcomes the magnetic pressure so that the gap is closed due to the hydrodynamical motion of the ejecta. The magnetar wind is trapped behind the ejecta, which heats and accelerates the ejecta, powering the merger-nova emission and the DNS merger afterglow emission. In the meantime, the initial jet energy would drive GRB afterglow emission. In the late stage, the ejecta becomes transparent and the magnetar wind still dissipates its energy and radiates X-ray photons, which freely escape the remnant and give rise to the re-brightening in the X-ray light curve.

In this work, we take $\eta_\nu = 0.3$ for both the extended emission and the late dissipated emission.

3.3. Magnetar-powered Merger-nova

Suppose the magnetar is surrounded by a quasi-spherical ejecta shell with mass $M_{\rm ej}$ and initial speed $v_{\rm i}$. A generic model for the dynamics and emission properties of the ejecta could be briefly summarized as follows (e.g., Yu et al. 2013).

Considering the energy injection from the magnetar and the energy dissipation through sweeping up the ambient medium, the total "effective kinetic energy" (total energy minus rest-mass energy) of the system can be expressed as

$$E = (\Gamma - 1)M_{\rm ej}c^2 + \Gamma E'_{\rm int} + \left(\Gamma^2 - 1\right)M_{\rm sw}c^2, \quad (5)$$

where Γ is the bulk Lorentz factor of the ejecta, $E'_{\rm int}$ is the internal energy measured in the comoving rest frame, $M_{\rm sw} = \frac{4\pi}{3}R^3 nm_p$ is the swept mass from the interstellar medium (with density n), and R is the radius of the ejecta. The dynamical evolution of the ejecta can be determined by

$$\frac{d\Gamma}{dt} = \frac{\frac{dE}{dt} - \Gamma\mathcal{D}\left(\frac{dE'_{\rm int}}{dt'}\right) - \left(\Gamma^2 - 1\right)c^2\left(\frac{dM_{\rm sw}}{dt}\right)}{M_{\rm ej}c^2 + E'_{\rm int} + 2\Gamma M_{\rm sw}c^2}, \quad (6)$$

where $\mathcal{D} = 1/[\Gamma(1-\beta)]$ is the Doppler factor with $\beta = \sqrt{1-\Gamma^{-2}}$. The comoving time dt' and luminosity L' can be connected with the observer's time and luminosity by $dt' = \mathcal{D}dt$ and $L' = \mathcal{D}^{-2}L$, respectively.

With energy conservation, we have

$$\frac{dE}{dt} = \xi L_{\rm sd} + \mathcal{D}^2 L'_{\rm ra} - \mathcal{D}^2 L'_{\rm e}. \quad (7)$$

The radioactive power $L'_{\rm ra}$ reads

$$L'_{\rm ra} = 4\times 10^{49} M_{\rm ej,-2}\left[\frac{1}{2} - \frac{1}{\pi}\arctan\left(\frac{t'-t'_0}{t'_\sigma}\right)\right]^{1.3} \ {\rm erg\ s^{-1}}, \quad (8)$$

with $t'_0 \sim 1.3$ s and $t'_\sigma \sim 0.11$ s (Korobkin et al. 2012). The radiated bolometric luminosity $L'_{\rm e}$ reads[11]

$$L'_{\rm e} = \begin{cases} \dfrac{E'_{\rm int}c}{\tau R/\Gamma}, & \tau > 1, \\ \dfrac{E'_{\rm int}c}{R/\Gamma}, & \tau < 1, \end{cases} \quad (9)$$

where $\tau = \kappa(M_{\rm ej}/V')(R/\Gamma)$ is the optical depth of the ejecta with κ being the opacity (Kasen & Bildsten 2010; Kotera et al. 2013).

[11] The energy loss due to shock emission is ignored here, as is usually done in GRB afterglow modeling.

The variation of the internal energy in the comoving frame can be expressed by (e.g., Kasen & Bildsten 2010)

$$\frac{dE'_{\rm int}}{dt'} = \xi \mathcal{D}^{-2} L_{\rm sd} + L'_{\rm ra} - L'_{\rm e} - \mathcal{P}' \frac{dV'}{dt'}, \quad (10)$$

where the radiation-dominated pressure can be estimated as $\mathcal{P}' = E'_{\rm int}/3\,V'$ and the comoving volume evolution can be fully addressed by

$$\frac{dV'}{dt'} = 4\pi R^2 \beta c, \quad (11)$$

together with

$$\frac{dR}{dt} = \frac{\beta c}{(1-\beta)}. \quad (12)$$

A full dynamical description of the system as well as the bolometric radiation luminosity can be easily obtained by solving the above differential equations. Assuming a blackbody spectrum for the thermal emission of the merger-nova for a certain observational frequency ν, the observed flux can be calculated as

$$F_\nu = \frac{1}{4\pi D_L^2 \max(\tau, 1)} \frac{8\pi^2 \mathcal{D}^2 R^2}{h^3 c^2} \frac{(h\nu/\mathcal{D})^4}{\exp(h\nu/\mathcal{D}kT') - 1}, \quad (13)$$

where h is the Planck constant.

3.4. GRB Afterglow Emission

The interaction between the initial launched jet and the ambient medium could generate a strong external shock, where particles are believed to be accelerated, giving rise to broadband synchrotron radiation (see Gao et al. 2013b for a review). The total effective kinetic energy of the jet and the medium can be expressed as

$$E = (\Gamma - 1) M_{\rm jet} c^2 + \left(\Gamma^2 - 1\right) M_{\rm sw} c^2, \quad (14)$$

where $M_{\rm sw} = 2\pi(1-\cos\theta)/3R^3 n m_p$, with θ being the half opening angle of the jet. The energy conservation law gives

$$\frac{d\Gamma}{dt} = \frac{-\left(\Gamma^2 - 1\right)\left(\frac{dM_{\rm sw}}{dt}\right)}{M_{\rm jet} + 2\Gamma M_{\rm sw}}, \quad (15)$$

where the energy loss due to shock emission is ignored.

In the comoving frame, the synchrotron radiation power at frequency ν' from electrons is given by (Rybicki & Lightman 1979)

$$P'_{\nu'} = \frac{\sqrt{3}\, q_{\rm e}^3 B'}{m_{\rm e} c^2} \int_{\gamma_{\rm e,m}}^{\gamma_{\rm e,M}} \left(\frac{dN'_{\rm e}}{d\gamma_{\rm e}}\right) F\left(\frac{\nu'}{\nu'_{\rm cr}}\right) d\gamma_{\rm e}, \quad (16)$$

where $q_{\rm e}$ is the electron charge, $\nu'_{\rm cr} = 3\gamma_{\rm e}^2 q_{\rm e} B'/(4\pi m_{\rm e} c)$ is the characteristic frequency of an electron with Lorentz factor $\gamma_{\rm e}$, B' is the comoving magnetic field strength, and

$$F(x) = x \int_x^{+\infty} K_{5/3}(k)\, dk, \quad (17)$$

with $K_{5/3}(k)$ being the Bessel function.

The comoving magnetic field strength B' could be estimated as

$$B' = \left(8\pi e_{\rm s} \epsilon_B\right)^{1/2}, \quad (18)$$

where $e_{\rm s}$ is the energy density in the shocked region and ϵ_B is the fraction of the shock energy density that goes into the magnetic field.

The distribution of the shock-accelerated electrons behind the blast wave is usually assumed to be a power-law function of electron energy,

$$\frac{dN'_{\rm e}}{d\gamma_{\rm e}} \propto \gamma_{\rm e}^{-p}, \quad \left(\gamma_{\rm e,m} \leqslant \gamma_{\rm e} \leqslant \gamma_{\rm e,M}\right). \quad (19)$$

Assuming that a constant fraction $\epsilon_{\rm e}$ of the shock energy is distributed to electrons, the minimum injected electron Lorentz factor can be estimated as

$$\gamma_{\rm e,m} = g(p)\, \epsilon_{\rm e} (\Gamma - 1) \frac{m_p}{m_{\rm e}}, \quad (20)$$

where the function $g(p)$ takes the form

$$g(p) \simeq \begin{cases} \dfrac{p-2}{p-1}, & p > 2; \\ \ln^{-1}(\gamma_{\rm e,M}/\gamma_{\rm e,m}), & p = 2. \end{cases} \quad (21)$$

The maximum electron Lorentz factor $\gamma_{\rm e,M}$ could be estimated by balancing the acceleration timescale and the dynamical timescale, i.e.,

$$\gamma_{\rm e,M} \sim \frac{\Gamma t q_{\rm e} B}{\zeta m_p c}, \quad (22)$$

where $\zeta \sim 1$ is a parameter that describes the details of acceleration. If the electron energy has a harder spectral index $1 < p < 2$, the minimum electron Lorentz factor would be derived as (Bhattacharya 2001; Dai & Cheng 2001)

$$\gamma_{\rm e,m} = \left(\frac{2-p}{p-1} \frac{m_p}{m_{\rm e}} \epsilon_{\rm e} (\Gamma - 1) \gamma_{\rm e,M}^{p-2}\right)^{1/(p-1)}. \quad (23)$$

With the dynamical description of the jet and these radiation equations, one can calculate the evolution of $P'_{\nu'}$. Assuming that this power is radiated isotropically, then the observed flux density at frequency $\nu = \mathcal{D}\nu'$ can be calculated as

$$F_\nu = \frac{\mathcal{D}^3}{4\pi D_L^2} P'_{\nu'}. \quad (24)$$

Note that in the following calculation, we neglect the sideway expansion of the jet (Rhoads 1999; Sari et al. 1999), but consider the jet break with an edge effect at a later time when $\Gamma^{-1} > \theta$ (Panaitescu et al. 1998).

3.5. DNS Merger Afterglow Emission

During the propagation of the ejecta, a strong external shock would also form upon interaction with the ambient medium. With a dynamical solution for the ejecta and the radiation equations (16)–(24), one can easily calculate the relevant broadband DNS merger afterglow emission (Gao et al. 2013a).

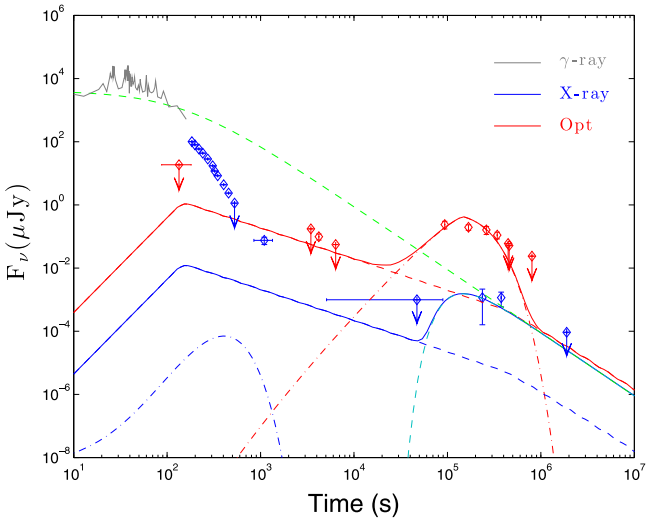

Figure 2. Modeling results for the broadband observations of GRB 080503. The data are taken from Hascoët et al. (2012), with blue denoting X-rays and red denoting optical. Blue and red dashed lines represent the GRB afterglow emission in the X-ray and optical bands, respectively; blue and red dot–dashed lines represent the merger-nova emission in the X-ray and optical band, respectively; the green dashed line denotes the evolution function of the magnetar spin-down radiation luminosity; the light blue dashed line denotes the late magnetar wind dissipation emission. The blue and red solid lines are final fitting lines for the X-ray and optical data, respectively.

4. APPLICATION TO GRB 080503

Considering the extremely deep limit for the host galaxy of GRB 080503, one plausible possibility is that GRB 080503 is at a moderately high redshift in a very underluminous galaxy, e.g., $z \approx 1$, comparable to the highest-z SGRBs (Perley et al. 2009). In the following, we adopt $z = 1$ and investigate the broadband data of GRB 080503 with the physical model proposed in the last section. We find that with all standard parameter values, the broadband data of GRB 080503 could be well explained. The fitting results (data from Hascoët et al. 2012) are presented in Figure 2 and the adopted parameter values are collected in Table 1. We briefly summarize the investigation results as follows.

1. The soft extended emission and the late X-ray excess peak could be connected with a magnetar spin-down luminosity evolution function, suggesting direct magnetic dissipation as the same underlying origin for these two observed components.
2. In the X-ray band, the contribution from the merger-nova and early GRB afterglow emission are overshadowed by the aforementioned direct magnetic dissipation component.
3. The early optical data can be explained by the GRB afterglow emission. The late optical data, including the re-brightening phase and the rapid decay feature, can be explained by the emission from a magnetar-powered merger-nova.
4. Both the late-time optical and X-ray data peak around the same time when $\tau = 1$, which is consistent with the argument that the late magnetar dissipation photons can travel freely after the ejecta becomes transparent. This powers the late X-ray excess.
5. For this particular event, the DNS merger afterglow emission is completely suppressed since the ejecta mass is relatively large so the ejecta is only mildly relativistic, and since the medium density is small. This emission component is not plotted in Figure 2.

Table 1
Parameters for Interpreting the Broadband Data of GRB 080503 by Assuming $z = 1$

Magnetar and Ejecta Parameters					
B (G)	P_i (ms)	R_s (cm)	M_{ej} ($M_\odot$)	v_i/c	κ (cm^2 g^{-1})
6×10^{15}	2	1.2×10^6	3×10^{-3}	0.2	10
Jet and Ambient Medium Parameters					
	E (erg)	Γ_0	n (cm^{-3})	θ (rad)	
	10^{51}	200	0.001	0.1	
Other Parameters					
ϵ_e	ϵ_B	p	ζ	ξ	η_γ
0.01	0.001	2.3	1	0.3	0.3

In this interpretation, we adopt the isotropic kinetic energy of the jet as 10^{51} erg, which is based on the total emission energy of the short spike and assume a factor of 20% for the γ-ray emission efficiency. The values for initial Lorentz factor (Γ_0) and half opening angle (θ) of the jet are chosen as 200 and 0.1, the values of which barely affect the final fitting results. To achieve the faintness of the GRB afterglow emission, a relatively low value for ambient medium density ($n = 0.001$ cm^{-3}) is required, suggesting that GRB 080503 may have a large offset relative to the center of its host galaxy, which in turn explains the extremely deep limit on its host at the afterglow location (since the system may have been kicked out far away from a host galaxy). The microphysics shock parameters (e.g., ϵ_e, ϵ_B, ζ, and p) are all set at their commonly used values in GRB afterglow modeling[12] (see Kumar & Zhang 2015 for a review). For the magnetar, a relatively large stellar radius $R_{s,6} = 1.2$ is adopted by considering a rapidly rotating supra-massive NS, and an initial spin period P_i is set at 2 ms by considering a mild angular momentum loss via strong gravitational radiation (Fan et al. 2013a). The dipolar magnetic field strength B is adopted as 6×10^{15} G, which is consistent with the suggested values by fitting the SGRB X-ray plateau feature (Rowlinson et al. 2013; Lü & Zhang 2014). For the ejecta, we take the standard values of mass ($M_{ej} \sim 10^{-3} M_\odot$) and initial velocity ($v_i = 0.2c$), and a relatively large value for the effective opacity $\kappa = 10$ cm^2 g^{-1}. The latter was suggested by recent works by considering the bound–bound, bound–free, and free–free transitions of ions (Kasen et al. 2013; Tanaka & Hotokezaka 2013). If the opacity has a smaller value (e.g., because of the intense neutrino emission from the proto-magnetar; Metzger and Fernández 2014), the same data can be interpreted by increasing the mass of the ejecta. For example, an equally good fit can be reached with $M_{ej} \sim 10^{-2} M_\odot$ for $\kappa = 1$ cm^2 g^{-1}. Finally, we assume that 30% of the wind energy is deposited into the ejecta, which is a nominal value suggested from previous works (Zhang & Yan 2011; Yu et al. 2013).

[12] Recently, Gao et al. (2015) performed a morphological analysis on GRB early optical afterglow light curves. To reproduce the current observational data, the preferred ϵ_e value is 0.01, which is adopted in this work.

5. CONCLUSION AND DISCUSSION

DNS mergers could leave behind a millisecond magnetar rather than a black hole. In this scenario, the spin-down of the magnetar provides an additional energy source in the merger remnant, which generates much richer EM signatures from the merger remnant system than the black hole scenario. In this work, we give a comprehensive description for all possible EM signals under the magnetar remnant scenario, invoking several emission sites to account for several emission components, i.e., the initially launched jet to produce the short spike in prompt emission; an external shock site for this jet component to account for part of the observed optical afterglow emission component; a magnetar wind internal dissipation site that accounts for the early soft extended emission, the high latitude tail emission, and the late X-ray re-brightening emission when the ejecta becomes transparent; an isotropic ejecta site that generates a magnetar-powered merger-nova emission; and finally the site where the ejecta interacts with the medium and powers the DNS merger afterglow emission.

We presnt detailed numerical methods to calculate these emission components and apply the model to investigate the broadband observations of GRB 080503. We find that the magentar remnant scenario could interpret the multi-band data of GRB 080503, including the extended emission and its re-brightening features in both X-ray and optical bands. In our calculation, we adopt $z = 1$ for GRB 080503, which could be a plausible assumption in view of both the extremely deep upper limit for the host galaxy flux and the observed redshift distribution of SGRBs. If our interpretation is correct, some important implications could be inferred.

1. GRB 080503 is of a DNS merger origin.
2. The post-merger remnant of this event is a stable magnetar, with an effectively polar cap dipole magnetic field of 6×10^{15} G and an initial period of 2 ms.
3. The late optical re-brightening is a magnetar-powered merger-nova. Since its emission is essentially isotropic, similar merger-novae are expected to be associated with NS–NS merger GW sources even without a short GRB association.
4. For this event, the ejected mass during the merger is estimated to be around $3 \times 10^{-3}\,M_{\odot}$.

To justify the assumption of $z = 1$, we also tested other redshift values (either smaller or larger than 1). We find that the fitting results are not sensitive to the redshift value, even though some parameters may vary within reasonable ranges.

In this work, we assume that the magetar wind is highly magnetized, i.e., with a high σ value. If, on the other hand, the wind contains a significant fraction of primary $e^{\pm}$ pairs, the magnetic wind may become leptonic-matter-dominated upon interaction with the ejecta, so a strong reverse shock can be developed, which would predict additional radiation signatures (Dai 2004; Wang & Dai 2013; Wang et al. 2015). Moreover, Metzger & Piro (2014) proposed that the large optical depth of $e^{\pm}$ pairs inside the ejecta shell could also suppress the efficiency for depositing the wind energy into the ejecta, which essentially corresponds to a reduced value of ξ in our model.

In our interpretation, we assume that the magnetar wind could leak out from the ejecta shell through the opening gap drilled by the initial jet, powering the extended emission. An alternative interpretation could be that the outflow from the magnetar wind itself may be collimated into a bipolar jet by its interaction with this ejecta (Bucciantini et al. 2012) and then power the extended emission (Metzger & Piro 2014). If this is the case, the real spin-down luminosity would be smaller than the extended emission luminosity due to the collimation effect, inferring a somewhat lower dipole field. However, such a collimation effect is only significant for a large ejecta mass (say $>10^{-2}\,M_{\odot}$), which should not affect the results in this work since the preferred ejecta mass for the case of GRB 080503 is relatively small ($\sim 10^{-3}\,M_{\odot}$).

Finally, it is worth pointing out that our described physical picture for the EM signatures from an NS–NS merger with a stable or supra-massive millisecond magnetar remnant could be applied to other cases of short GRBs and also cases when the jet beams away from Earth. A systematic study of extended emission and internal plateau emission from short GRBs (Lü et al. 2015) revealed many plateaus followed by a rapid decay. It would be interesting to systematically apply the model to these GRBs to constrain the model parameters. In most cases, no X-ray re-brightening is observed, which suggests that the magnetar is likely supra-massive, and has collapsed into a black hole before the ejecta becomes transparent. In the future, off-axis X-ray transients may be discovered to be associated with GW events due to NS–NS mergers (Zhang 2013). Applying our model to these events can give more detailed predictions on the brightness of these X-ray transients, which is valuable for searching for EM counterparts of GW signals in the Advanced LIGO/Virgo era.

This work is supported by the National Basic Research Program ("973" Program) of China (grants 2014CB845800 and 2013CB834900), the National Natural Science Foundation of China (grant Nos. 11322328, 11033002, and 11433009). H. G. acknowledges support by NASA NNX 13AH50G. X.F.W. is partially supported by the One-Hundred-Talents Program, the Youth Innovation Promotion Association, and the Strategic Priority Research Program "The Emergence of Cosmological Structures" (grant No. XDB09000000) of the Chinese Academy of Sciences, and the Natural Science Foundation of Jiangsu Province (grant No. BK2012890).

APPENDIX

The initial jet launched during the early accretion phase that powers the short GRB may have drilled a bipolar cavity in the ejecta. The subsequent magnetar wind following the short GRB also penetrates through this cavity and powers the extended emission. During this phase, the ram pressure around the cavity due to the dynamical motion of the ejecta would be initially balanced by the transverse magnetic pressure in the magnetar wind, i.e.,

$$\frac{L_{\rm sd,i}\,\phi}{4\pi R^2 c} \sim \frac{M_{\rm ej} v^2}{4\pi R^2 \Delta}, \tag{25}$$

where c is the speed of light, ϕ is the transverse magnetic pressure fraction, R is the radius of the ejecta, and Δ is the thickness of the ejecta shell. Under this condition, the corresponding fluid speed in the transverse direction due to

dynamical motion of the ejecta can be estimated as

$$v = \left(\frac{L_{\rm sd,i}\phi\Delta}{M_{\rm ej}c}\right)^{1/2} \approx 0.04c\, R_{\rm s,6}^{3} B_{15} P_{\rm i,-3}^{-2} M_{\rm ej}^{-1/2} v_{\rm i,10}^{1/2} \phi^{1/2}, \quad (26)$$

where $\Delta = v_{\rm i}\Delta t$, with $v_{\rm i} \sim 10^{10}\,{\rm cm\,s^{-1}}$ and $\Delta t = 1\,{\rm s}$ (Bucciantini et al. 2012). When $t > t_{\rm sd}$, the magnetic pressure quickly drops, so the cavity would be gradually closed on a timescale

$$t_{\rm close} \approx \frac{\beta_{\rm sd} t_{\rm sd} c\theta}{v_{\rm s}}, \quad (27)$$

where θ is the jet opening angle and $\beta_{\rm sd}$ is the ejecta radial speed at $t_{\rm sd}$. Through energy conservation, we obtain

$$\beta_{\rm sd} = \min\left[1, \left(\frac{\xi E_{\rm rot}}{M_{\rm ej}c^2}\right)^{1/2}\right]. \quad (28)$$

For the cases with $\beta_{\rm sd}$ not close to unity (such as the case for GRB 080503 with $\beta_{\rm sd} \sim 0.5$), we have

$$t_{\rm close} \approx 1.5 \times 10^4\,{\rm s}\, R_{\rm s,6}^{-9} B_{15}^{-3} P_{\rm i,-3}^{3} \theta_{-1} v_{\rm i,10}^{-1/2} \xi^{1/2} \phi^{-1/2}. \quad (29)$$

The total timescale for the extended emission can be estimated as

$$t_{\rm ee} = t_{\rm sd} + t_{\rm close}. \quad (30)$$

With the parameters adopted to interpret the data of GRB 080503, we have $t_{\rm ee} \approx 74.4 + 157.3(\phi/0.25)^{-1/2}$ s, which is consistent with the stopping time of extended emission (232 s), provided that the $\phi \sim 1/4$ of the magnetic pressure concentrates in the transverse direction.

REFERENCES

Abbott, B. P., Abbott, R., Adhikari, R., et al. 2009, RPPh, 72, 076901
Acernese, F., Alshourbagy, M., Amico, P., et al. 2008, CQGra, 25, 114045
Aloy, M. A., Janka, H.-T., & Müller, E. 2005, A&A, 436, 273
Barnes, J., & Kasen, D. 2013, ApJ, 775, 18
Barthelmy, S. D., Cannizzo, J. K., Gehrels, N., et al. 2005, ApJL, 635, L133
Bauswein, A., Goriely, S., & Janka, H.-T. 2013, ApJ, 773, 78
Berger, E. 2014, ARA&A, 52, 43
Berger, E., Fong, W., & Chornock, R. 2013, ApJL, 774, L23
Bhattacharya, D. 2001, BASI, 29, 107
Bloom, J. S., Prochaska, J. X., Pooley, D., et al. 2006, ApJ, 638, 354
Bucciantini, N., Metzger, B. D., Thompson, T. A., & Quataert, E. 2012, MNRAS, 419, 1537
Burrows, D. N., Grupe, D., Capalbi, M., et al. 2006, ApJ, 653, 468
Campana, S., Mangano, V., Blustin, A. J., et al. 2006, Natur, 442, 1008
Dai, Z. G. 2004, ApJ, 606, 1000
Dai, Z. G., & Cheng, K. S. 2001, ApJL, 558, L109
Dai, Z. G., Wang, X. Y., Wu, X. F., & Zhang, B. 2006, Sci, 311, 1127
de Pasquale, M., Schady, P., Kuin, N. P. M., et al. 2010, ApJL, 709, L146
Dessart, L., Ott, C. D., Burrows, A., Rosswog, S., & Livne, E. 2009, ApJ, 690, 1681
Eichler, D., Livio, M., Piran, T., & Schramm, D. N. 1989, Natur, 340, 126
Fan, Y.-Z., & Xu, D. 2006, MNRAS, 372, L19
Fan, Y.-Z., Wu, X.-F., & Wei, D.-M. 2013a, PhRvD, 88, 067304
Fan, Y.-Z., Yu, Y.-W., Xu, D., et al. 2013b, ApJL, 779, L25
Fernández, R., & Metzger, B. D. 2013, MNRAS, 435, 502
Gao, H., Ding, X., Wu, X.-F., Zhang, B., & Dai, Z.-G. 2013a, ApJ, 771, 86
Gao, H., Lei, W.-H., Zou, Y.-C., Wu, X.-F., & Zhang, B. 2013b, NewAR, 57, 141
Gao, H., Wang, X.-G., Mészáros, P., et al. 2015, ApJ, submitted
Gao, W.-H., & Fan, Y.-Z. 2006, ChJAA, 6, 513
Giacomazzo, B., & Perna, R. 2013, ApJL, 771, L26
Hascoët, R., Daigne, F., & Mochkovitch, R. 2012, A&A, 542, L29
Hotokezaka, K., Kiuchi, K., Kyutoku, K., et al. 2013, PhRvD, 87, 024001
Kasen, D., & Bildsten, L. 2010, ApJ, 717, 245
Kasen, D., Badnell, N. R., & Barnes, J. 2013, ApJ, 774, 25
Kocevski, D., Thöne, C. C., Ramirez-Ruiz, E., et al. 2010, MNRAS, 404, 963
Korobkin, O., Rosswog, S., Arcones, A., & Winteler, C. 2012, MNRAS, 426, 1940
Kotera, K., Phinney, E. S., & Olinto, A. V. 2013, MNRAS, 432, 3228
Kulkarni, S. R. 2005, arXiv:astro-ph/0510256
Kumar, P., & Panaitescu, A. 2000, ApJL, 541, L51
Kumar, P., & Zhang, B. 2015, Phys. Rep., 561, 1
Kuroda, K., & LCGT Collaboration 2010, CQGra, 27, 084004
Lee, W. H., Ramirez-Ruiz, E., & López-Cámara, D. 2009, ApJL, 699, L93
Li, L.-X., & Paczyński, B. 1998, ApJL, 507, L59
Lü, H.-J., & Zhang, B. 2014, ApJ, 785, 74
Lü, H.-J., Zhang, B., Lei, W.-H., Li, Y., & Lasky, P. D. 2015, ApJ, 805, 89
Metzger, B. D., & Berger, E. 2012, ApJ, 746, 48
Metzger, B. D., & Fernández, R. 2014, MNRAS, 441, 3444
Metzger, B. D., Martínez-Pinedo, G., Darbha, S., et al. 2010, MNRAS, 406, 2650
Metzger, B. D., & Piro, A. L. 2014, MNRAS, 439, 3916
Metzger, B. D., Quataert, E., & Thompson, T. A. 2008, MNRAS, 385, 1455
Nakar, E., & Piran, T. 2011, Natur, 478, 82
Narayan, R., Paczynski, B., & Piran, T. 1992, ApJL, 395, L83
Norris, J. P., & Bonnell, J. T. 2006, ApJ, 643, 266
Paczýnski, B. 1986, ApJL, 308, L43
Paczýnski, B. 1991, AcA, 41, 257
Panaitescu, A., Mészáros, P., & Rees, M. J. 1998, ApJ, 503, 314
Perley, D. A., Cenko, S. B., Bloom, J. S., et al. 2009, AJ, 138, 1690
Piran, T., Nakar, E., & Rosswog, S. 2013, MNRAS, 430, 2121
Rezzolla, L., Giacomazzo, B., Baiotti, L., et al. 2011, ApJL, 732, L6
Rhoads, J. E. 1999, ApJ, 525, 737
Rosswog, S., Piran, T., & Nakar, E. 2013, MNRAS, 430, 2585
Rosswog, S., Ramirez-Ruiz, E., & Davies, M. B. 2003, MNRAS, 345, 1077
Rowlinson, A., O'Brien, P. T., Metzger, B. D., Tanvir, N. R., & Levan, A. J. 2013, MNRAS, 430, 1061
Rowlinson, A., O'Brien, P. T., Tanvir, N. R., et al. 2010, MNRAS, 409, 531
Rybicki, G. B., & Lightman, A. P. 1979, in Radiative Processes in Astrophysics (New York: Wiley), 393
Sari, R., Piran, T., & Halpern, J. P. 1999, ApJL, 519, L17
Shibata, M., Taniguchi, K., & Uryū, K. 2005, PhRvD, 71, 084021
Tanaka, M., & Hotokezaka, K. 2013, ApJ, 775, 113
Tanvir, N. R., Levan, A. J., Fruchter, A. S., et al. 2013, Natur, 500, 547
Wang, L.-J., & Dai, Z.-G. 2013, ApJL, 774, L33
Wang, L.-J., Dai, Z.-G., & Yu, Y.-W. 2015, ApJ, 800, 79
Wu, X.-F., Gao, H., Ding, X., et al. 2014, ApJL, 781, L10
Yang, B., Jin, Z.-P., Li, X., et al. 2015, arXiv:1503.07761
Yu, Y.-W., Li, S.-Z., & Dai, Z.-G. 2015, ApJL, 806, L6
Yu, Y.-W., Zhang, B., & Gao, H. 2013, ApJL, 776, L40
Zhang, B.-B., Liang, E.-W., & Zhang, B. 2007, ApJ, 666, 1002
Zhang, B.-B., Zhang, B., Liang, E.-W., & Wang, X.-Y. 2009, ApJL, 690, L10
Zhang, B., & Yan, H. 2011, ApJ, 726, 90
Zhang, B. 2013, ApJL, 763, L22
Zhang, D., & Dai, Z. G. 2008, ApJ, 683, 329
Zhang, D., & Dai, Z. G. 2009, ApJ, 703, 461
Zhang, D., & Dai, Z. G. 2010, ApJ, 718, 841